Fast x-ray spectroscopy study of ethene on clean and SO_4 precovered Pt{111}

Adam F. Lee, and Karen Wilson

ARTICLES YOU MAY BE INTERESTED IN

Ethene adsorption and dehydrogenation on clean and oxygen precovered Ni(111) studied by high resolution x-ray photoelectron spectroscopy
The Journal of Chemical Physics **133**, 014706 (2010); https://doi.org/10.1063/1.3456732

Hybrid $Fe_3O_4 / GaAs(100)$ structure for spintronics
Journal of Applied Physics **97**, 10C313 (2005); https://doi.org/10.1063/1.1857432

A catalytic reactor for the trapping of free radicals from gas phase oxidation reactions
Review of Scientific Instruments **81**, 104102 (2010); https://doi.org/10.1063/1.3492247

Direct observation of surface reactions by scanning tunneling microscopy: Ethylene→ethylidyne→carbon particles→graphite on Pt(111)
The Journal of Chemical Physics **97**, 6774 (1992); https://doi.org/10.1063/1.463655

Ethylene π species on bare and cesiated Pt(111) surfaces
Journal of Vacuum Science & Technology A **7**, 3312 (1989); https://doi.org/10.1116/1.576142

A detailed analysis of vibrational excitations in x-ray photoelectron spectra of adsorbed small hydrocarbons
The Journal of Chemical Physics **125**, 204706 (2006); https://doi.org/10.1063/1.2397678

Fast x-ray spectroscopy study of ethene on clean and SO$_4$ precovered Pt{111}

Adam F. Lee[a)]
Department of Chemistry, University of Hull, Hull HU6 7RX, United Kingdom

Karen Wilson
Department of Chemistry, University of York, York YO10 5DD, United Kingdom

The adsorption and decomposition of ethylene over a Pt{111} single crystal surface has been investigated by fast x-ray spectroscopy. At 100 K ethene displays precursor-mediated adsorption kinetics, adopting a single environment with a saturation C$_2$H$_4$ coverage of 0.25 ML and binding energy of 283.2 eV. Thermal decomposition proceeds above 240 K via dehydrogenation to ethylidyne with an activation barrier of 57 ± 3 kJ mol^{-1} and preexponential factor $\nu = 1 \times 10^{10 \pm 0.5}$ s^{-1}. Site-blocking by preadsorbed SO$_4$ reduces the saturation ethene coverage but induces a new, less reactive π-bonded ethene species centered around 283.9 eV, which in turn decomposes to ethylidyne at 350 K. © *2003 American Vacuum Society.*
[DOI: 10.1116/1.1559923]

I. INTRODUCTION

Improved mechanistic understanding of hydrocarbon chemistry over transition metal surfaces is central to the design of new and more efficient heterogeneously catalyzed organic transformations. Of particular interest is the interaction of alkenes with poison or promoter species over metal surfaces. Previous studies have addressed the interaction of ethene with alkali metals or oxygen.[1–3] Other important surface modifiers are sulphoxy species prevalent in Pt doped SO$_4$/ZrO$_2$[4] catalysts for alkene isomerization and Pt/Al$_2$O$_3$ automotive pollution control catalysts for alkene combustion. Here we report the application of fast x-ray photoelectron spectroscopy (XPS) as an *in situ* chemically specific probe to study the adsorption and reaction of ethene over clean and sulphated Pt{111}.

The interaction of ethene with Pt{111} surfaces is frequently used as a model system to understand alkene hydrogenation/dehydrogenation processes in heterogeneous catalysis, and as such has been the subject of many investigations. Bonding of ethene to metal surfaces largely occurs via an electronic interaction between the metal *d* band and the filled π or vacant π^* orbitals of the C=C bond. A range of techniques including reflection absorption infrared spectroscopy,[5] high-resolution electron energy-loss spectra,[3] near edge x-ray absorption fine structure (NEXAFS),[6] and temperature programmed desorption (TPD)[7] have been applied to studying the adsorption geometry and decomposition pathways of ethene on Pt{111}, and it is generally agreed that below 52 K ethene retains its sp^2 character, adsorbing with the C=C bond parallel to the surface through a weak π donor interaction.[8] However, for temperatures above 90 K chemisorption occurs with electron transfer from the Pt into the π^* orbital inducing significant rehybridization of the π bond and the formation of a di-σ bound species. Calculations based on structural and vibrational analyses show that in this di-σ adsorption geometry ethene is almost sp^3 hybridized[9] with the C–C bond length increased from 1.34 to 1.49 Å.[6] Recent density functional theory (DFT) calculations suggest this is consistent with adsorption at a bridge site.[10] On warming the surface to above 230 K a fraction of the di-σ ethene is observed to desorb prior to dehydrogenation of the remaining species to form an ordered (2×2) overlayer[3] of a perpendicular ethylidyne species. Low-energy electron diffraction (LEED)-IV[11] measurements and DFT[10] calculations indicate that occupation of the fcc hollow site favored. Above 500 K further dehydrogenation of ethylidyne occurs resulting in the formation of CH fragments and eventually graphitic carbon.

This article reports the application of fast XPS to studying the adsorption and reactivity of ethene over clean and sulphated Pt{111} surfaces. In a single experiment simultaneous real time observation of both surface reactant and product distributions is permitted directly from their C 1*s* XP spectra. In addition to kinetic parameters for the ethylene→ethylidyne transformation, the threshold temperature for dehydrogenation and surface coverages of intermediates will be reported. This work is complimentary to earlier studies using LITDS,[12,13] vibrational spectroscopy,[14] T-NEXAFS,[15] and static secondary ion mass spectroscopy[16] to follow the kinetics of ethene dehydrogenation over clean Pt{111}. Evidence is also presented for a direct, mutual interaction between ethene and SO$_4$ which hinders the dehydrogenation pathway.

II. EXPERIMENT

Measurements were carried out at the SuperESCA beamline of the ELETTRA synchrotron radiation source using a Pt{111} single-crystal sample prepared by standard procedures and maintained under ultrahigh vacuum ($\sim 1 \times 10^{-10}$ Torr). Quoted exposures are given in langmuirs (1 L = 1

[a)]Author to whom correspondence should be addressed; electronic mail: a.f.lee@chem.hull.ac.uk
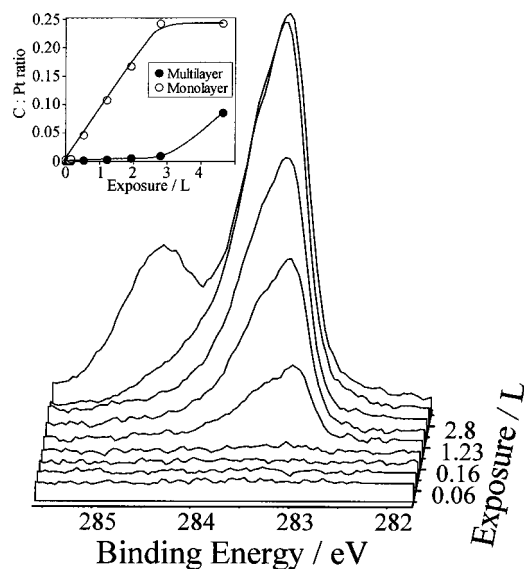
FIG. 1. C $1s$ fast XP spectra during C_2H_4 adsorption on clean Pt{111} at 95 K. Inset shows fitted component intensities.

FIG. 2. C $1s$ fast XP temperature programmed reaction spectra from a saturation C_2H_4 adlayer on clean Pt{111}. Inset shows corresponding image plot.

$\times 10^{-6}$ Torr s^{-1}) and are uncorrected for ion-gauge sensitivity. The crystal was held at 90 K during dosing. Temperature programmed reaction data were acquired by application of a linear heating ramp ($\sim$0.4 K s^{-1}) to the exposed sample. Ethene (Air Liquide 99%) was used without purification. Sample dosing was performed by backfilling the vacuum chamber.

Carbon $1s$ and sulphur $2p$ XP spectra, referenced to the Fermi level, were acquired at a photon energy of 398 eV and energy resolution of $\sim$100 meV. Individual spectra were acquired approximately every 30 s during fast XP measurements. The background-subtracted spectra were fitted using a Doniach–Sunjic function convoluted with a Gaussian. Fitting parameters for molecular ethene were determined from the 100 K clean surface uptake, while those for ethylidyne were derived from a 300 K saturation ethene exposure and for carbon from a 900 K annealed surface. The same surfaces were used to calculate the corresponding absorption cross sections based on their known surface coverages. Photoelectron spectra were measured at normal emission, using a 96-channel double-pass hemispherical analyzer. Absolute carbon coverages were determined by calibration with CO.

III. RESULTS AND DISCUSSION

A. Ethene adsorption over Pt{111}

The low temperature adsorption of ethene over the clean Pt{111} surface was followed by fast XPS at 95 K (Fig. 1). It is widely accepted that under these conditions C_2H_4 molecularly chemisorbs in an extensively rehybridized di-σ geometry and indeed at low coverages a single C $1s$ feature was observed centered around 283.2 eV. This state grew linearly with exposure up to 2.5 L (Fig. 1 inset) indicative of precursor-mediated adsorption of molecular ethene. The saturation coverage $\theta(C_2H_4) = 0.25$ ML in accord with previous LEED and TDS estimates.[17] The ethene line shape is
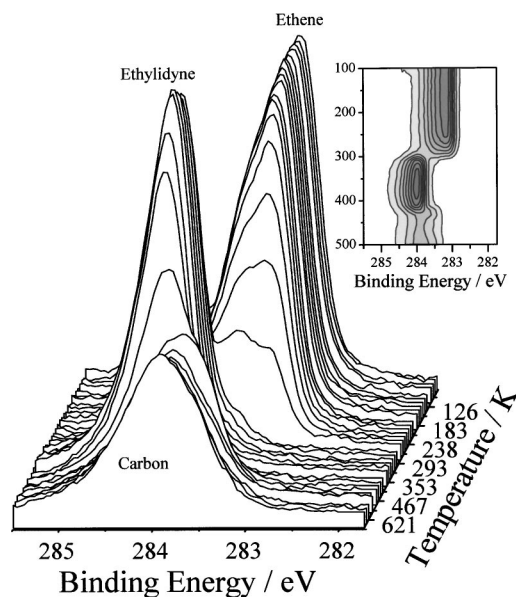
analogous to that observed in the gas phase and for adsorption on Rh{111},[18] and contains a high binding energy shoulder centered $\sim$283.5 eV due to internal molecular vibrational modes. There was no evidence for population of the more weakly bound π-bonded state, which is stabilized at lower temperatures[8] or high background ethylene pressures.[19] Higher exposures resulted in the growth of a second state with a similar line shape at $\sim$284.5 eV which increased continuously indicative of the physisorbed multilayer.

B. Ethene decomposition over Pt{111}

Figure 2 follows the subsequent thermal decomposition of a saturation C_2H_4 adlayer on clean Pt{111} during continuous heating. Above 110 K the multilayer desorbed leaving only chemisorbed di-σ bound ethene. The monolayer remained stable up to $\sim$240 K, above which the C_2H_4 intensity decreased rapidly with the concomitant appearance of a new higher binding energy feature at 284.1 eV. This new state has a sharper linewidth than ethene and is stable up to $\sim$400 K. At $\sim$240 K it is known that most of the C_2H_4 adlayer desorbs with the remainder dehydrogenating via the loss of one hydrogen atom to form surface ethylidyne ($Pt_3\equiv C-CH_3$).[3,5–7] It is thus reasonable to associate this peak shift and narrowing with ethylidyne formation (the only surface intermediate isolated to date in ethylene decomposition over Pt{111}). In contrast to recent studies of ethylidyne on Rh{111}[18] the inequivalent carbons are not resolved, although the intensity of the outer (methyl) carbon is strongly influenced by photoelectron diffraction effects. Higher temperatures result in loss of this ethylidyne state and a progressive shift in the peak maximum to lower binding energy with associated line broadening. These changes reflect further dehydrogenation coupled with C–C cleavage and the formation
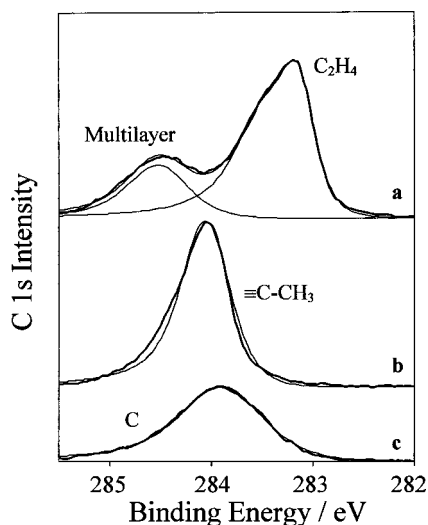
FIG. 3. Deconvoluted C $1s$ components from a saturation C_2H_4 adlayer on clean Pt{111} annealed to (a) 100 K, (b) 300 K, and (c) 680 K.

of CH_x fragments and subsequent complete dehydrogenation to residual surface carbon species at 283.9 eV.

The temperature programmed reaction spectra in Fig. 2 were successfully fitted using components corresponding to first layer and multilayer ethene, ethylidyne, and carbon shown in Fig. 3. Figure 4 shows the resultant fitted intensities normalized to their corresponding absorption cross sections and raises several points. First chemisorbed ethene begins desorbing at 230 K, just below the threshold reaction temperature for ethylidyne formation of 250 K. This is consistent with the model that some ethene desorption is required to liberate sufficient free sites for the initial dehydrogenation step to ethylidyne via either a vinyl or ethylidene intermediate.[12,13] The maximum ethylidyne coverage of 0.11 ML equates to a yield of 45% in accord with TPD studies which indicate ~56% of ethene desorbs intact from Pt{111} in accord with the TPD studies of Windham et al.[1] Second it is important to note that only one chemically distinct form of chemisorbed ethene is present on the surface at all temperatures. There is considerable speculation regarding the nature of the reversibly and irreversibly bound (reactive)
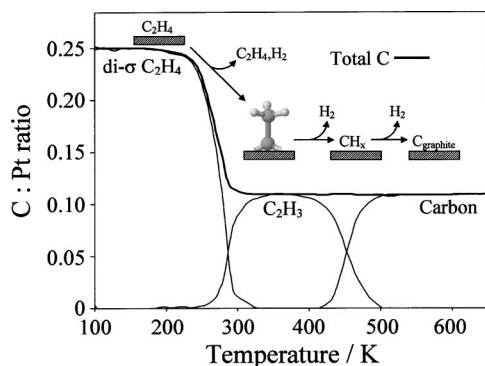
FIG. 4. Fitted C $1s$ intensities as a function of temperature for a saturation C_2H_4 adlayer on Pt{111}. The total integrated C signal is also shown.
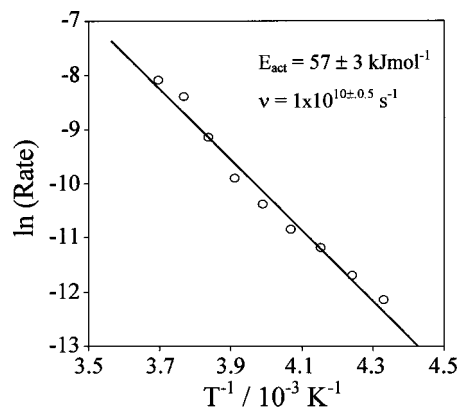
FIG. 5. Arrhenius plots of ethylidyne formation from a saturation reacting C_2H_4 adlayer on Pt{111}.

ethene, however, these species are indistinguishable by our high-resolution XPS suggesting a common adsorption geometry/degree of hybridization. A leading-edge analysis of the ethylidyne reaction profile (Fig. 5) reveals first-order kinetics with an activation barrier of 57 ± 3 kJ mol^{-1} and pre-exponential factor $\nu = 1 \times 10^{10 \pm 0.5}$ s^{-1}. These values are in good agreement with the Fourier transform infrared study of Moshin et al.[14] with $\Delta E_{act} = 59 \pm 4$ kJ mol^{-1} and $\nu = 1 \times 10^{10}$ s^{-1}, and the Fourier transform infrared reflection absorption study by Erley et al.[13] which likewise found ethylidyne formation was strictly first-order independent of ethene coverage with $\Delta E_{act} = 67 \pm 2$ kJ mol^{-1} and $\nu = 6 \times 10^{10 \pm 0.33}$ s^{-1}. It is important to note these values are significantly lower than those inferred from ethene decomposition by Salmeron and Somorjai[7] and by Windham et al.[1,20] using TDS, wherein H_2 desorption was assumed reaction-rate limited.

C. Ethene adsorption over sulphated Pt{111}

Ethene adsorption was also explored over sulphated Pt{111} to investigate the influence of coadsorbed sulphoxy species which are commonly occurring poisons during hydrocarbon combustion. A pure sulphate adlayer was prepared by adsorbing 12 L of SO_2 onto oxygen presaturated Pt{111} at 100 K, and subsequently annealing to room temperature as previously reported.[21] The resulting SO_4 coverage was 0.25 ML. Figure 6 compares the C $1s$ spectra following a 2 L C_2H_4 exposure (below the multilayer threshold) at 95 K over the sulphated surface with that from the corresponding clean surface. On the sulphated surface a small shift in the peak maximum to around 283.3 eV is apparent and the line shape cannot be reproduced using only a di-σ ethene state. A good fit could be achieved, however, by including an additional component with the same parameters as molecular ethene but with a higher binding energy of 283.9 eV.

A clear candidate for a second such state is a π-bound species as has been reported on Pt{111} at low temperatures and high pressures. Such π-bound ethene remains essentially sp^2 hybridized and adsorbs reversibly with a π-donor/ π^*-acceptor interaction with the clean platinum surface.[1]
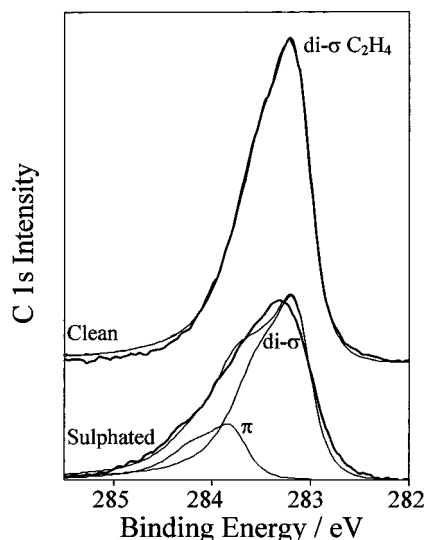
FIG. 6. Comparison of deconvoluted C 1s XP spectra of 2 L C_2H_4 on clean and SO_4-precovered Pt{111}.

FIG. 7. S 2p fast XP spectra during C_2H_4 adsorption over sulphated Pt{111} at 95 K. $\theta(SO_4)=0.25$ ML. Inset shows spectral deconvolution.

Electropositive/negative coadsorbates have been show to promote the formation of π-bonded ethene over Pt{111} via surface-mediated charge transfer. For example, K and Cs suppress the strong Pt–C covalent bonds normally formed by di-σ ethene, while C and O enhance π donation from the C=C bond into Pt d orbitals but suppress back donation from the metal to the π^* orbital. In all these cases π-bonded ethene remained weakly adsorbed, desorbing <120 K, whereas sulphate, as we will show later, exerts a far greater stabilizing influence. It is also important to note that the coexistence of distinct ethene adsorption states suggests surface sulphate exerts a localized not global influence on Pt{111}.

The total saturation ethene coverage is reduced by ~25% over the sulphated surface in comparison with adsorption over bare Pt{111} reflecting the loss of available metal sites. Since the surface comprises a roughly equal mix of ethene and sulphate, yet only around one-third of ethene is perturbed by proximity to sulphate groups, a likely scenario is that the surface comprises mutually exclusive islands of each coadsorbate and not a mixed adlayer. Sulphate-induced ethene perturbation would thus be confined to their contacted perimeters, with islands possessing a high perimeter:area ratio. The absence of ordered LEED structures is consistent with formation of such small ethene islands across the Pt{111} surface.

Further evidence for an interaction between coadsorbed sulphate and ethene is provided by the corresponding S 2p XP spectra recorded during low temperature ethene adsorption. Figure 7 shows a strong doublet at 167 eV ($p_{3/2}$ component), with a spin-orbit splitting of 1.15 eV, arising from SO_4 over clean Pt{111}. A small fraction of unoxidized SO_2 is also present at 166 eV but represents <15% of the total sulphoxy species and plays a negligible role in the surface chemistry. Subsequent ethene adsorption increases the SO_x binding energies by ~0.3 eV. This shift occurs over precisely the coverage regime in which the perturbed ethene state is
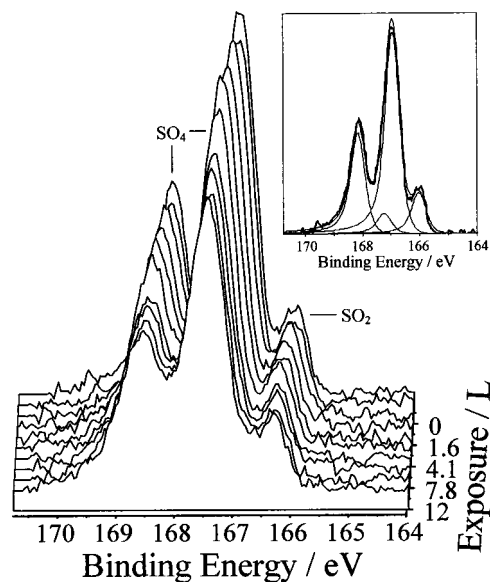
formed (Fig. 8) and is not associated with either di-σ or multilayer ethene. A similar SO_4 peak shift of 0.2 eV was observed following propene coadsorption over Pt{111}.[22] The origin of this shift is not certain but is consistent with a change in substrate-related charge-transfer into the sulphate σ^* and π^* LUMOs. Recent *ab initio* cluster calculations of sulphate adsorption on bare transition metals show the sulphate HOMOs are delocalized through the oxygen atoms, which push charge into the surface. Conversely the sulphate LUMOs are localized on the electron-deficient sulphur atom which accepts charge from the surface.[23] The magnitude of this sulphur back bonding increases with the overall sulphate adsorption strength and thus coordination number. Mono-, bi-, and tridentate sulphate adsorption geometries are all possible, however, cluster calculations suggest coordination via three oxygen atoms is strongly favored over Ag{111} and Au{111} surfaces. In the present case surface crowding following ethene adsorption on Pt{111} may force preadsorbed sulphate to switch from a sterically demanding polydentate geometry to a more weakly bound monodentate geometry.
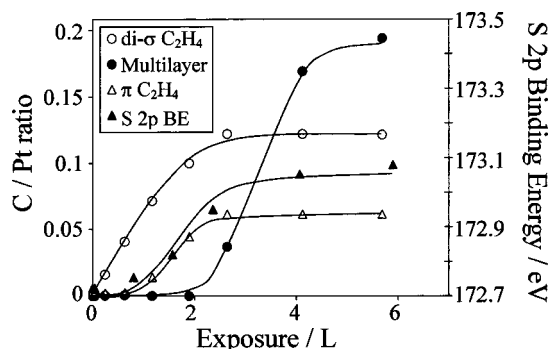
FIG. 8. Fitted C 1s intensities as a function of C_2H_4 exposure over SO_4-precovered Pt{111}. The binding energy is shown for comparison.
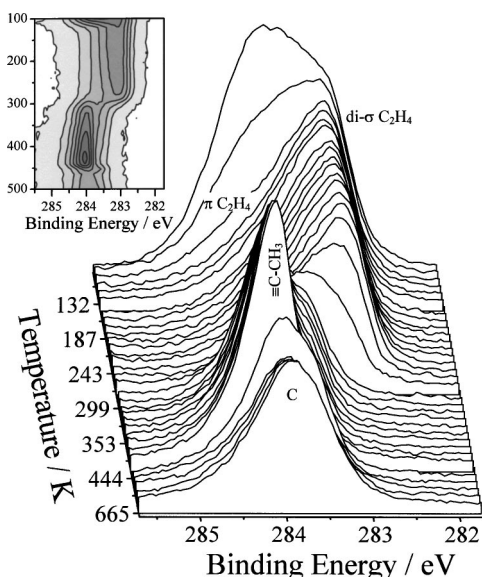
FIG. 9. C 1s fast XP temperature programmed reaction spectra from a saturation C_2H_4 adlayer on SO_4-precovered Pt{111}. Inset shows corresponding image plot.

FIG. 10. Fitted C 1s intensities as a function of temperature for a saturation C_2H_4 adlayer on SO_4-precovered Pt{111}. The total integrated C signal is also shown.

The corresponding reduction in Pt–S back bonding, predicted to be around 0.05 eV, could account for the increased S 2p binding energy.

D. Ethene decomposition over sulphated Pt{111}

Temperature programmed reaction spectra acquired during continuous heating of a saturated C_2H_4 adlayer over sulphated Pt{111} are shown in Fig. 9. The multilayer was fully desorbed above 110 K leaving the two chemisorbed ethene species responsible for a broad asymmetric peak from 282 to 284 eV. As over clean Pt{111}, the di-σ ethene adlayer was stable up to ~250 K. Further heating triggered rapid decay of this principal, unperturbed ethene component at 283 eV and a concomitant appearance of a new state at 284.1 eV corresponding to ethylidyne formation. However, significant intensity is retained ~283.5 eV until temperatures in excess of 350 K, at which point only ethylidyne is present. Higher temperatures result in complete decomposition to carbon as over the clean surface.

Figure 10 shows the result of deconvolution and peak fitting of the C 1s spectra. First it is important to note that the onset temperature for desorption and subsequent dehydrogenation of the di-σ state characteristic of the clean surface is unchanged. As over Pt{111} the desorption of ~50% of this di-σ ethene frees up sufficient bare sites to trigger transformation of the remainder to ethylidyne. In contrast the sulphate perturbed species remains stable to >350 K (with a corresponding $\Delta E_{act} = 100 \pm 5$ kJ mol^{-1}); its subsequent (complete) reaction to ethylidyne confirms that C_2 character was retained upon adsorption. The strength of alkene chemisorption and reactivity can be interpreted in terms of the Dewar–Chatt–Duncanson model, in which a synergistic π-donor, π*-back-bonding interaction occurs between the alkene and the surface. Strong back-bonding interactions re-

hybridize the C–C bond with a corresponding increase in M–C bond strength[9,24] and reactivity as for di-σ ethene. Sulphate should act as a net electron donor[23] to a metal surface, and thus suppress the corresponding ethene→Pt{111} donor interaction, decreasing the extent of ethene rehybridization. This in turn is expected to strengthen the C–H bond (ranging from 410 to 431 kJ mol^{-1} for gas-phase ethane and ethene, respectively[25]) and lower the corresponding reactivity over Pt{111}. This model is consistent with the higher threshold reaction temperature observed for ethylidyne formation from our proposed sp^2-like π-C_2H_4 species.
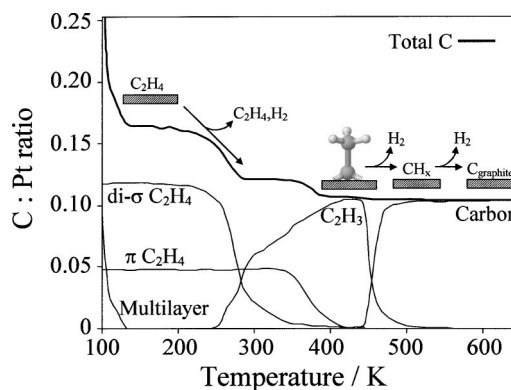
IV. CONCLUSIONS

(1) Ethene adopts a single adsorption environment over Pt(111) at 100 K with a characteristic binding energy of 283.2 eV and a saturation coverage of 0.25 ML.

(2) Approximately 44% of a saturation ethene adlayer dehydrogenates to form ethylidyne over clean Pt{111}, proceeding with an activation barrier of 57 ± 3 kJ mol^{-1} and pre-exponential factor $\nu = 1 \times 10^{10 \pm 0.5}$ s^{-1}. Ethylidyne possesses a narrow line shape centered around 284.1 eV.

(3) Preadsorbed sulphate reduces the saturation coverage of ethene over Pt{111} and promotes the formation of a less rehybridized π-bound species shifted to higher binding energy by 0.7 eV. This π-ethene state is populated near saturation coverage and correlates with an increase in the SO_4 (S 2p) binding energy suggesting a localized interaction between the coadsorbates.

(4) The decomposition of both di σ- and π-bound ethene proceeds via an isolable ethylidyne intermediate, however, SO_4 enhances the thermal stability of ethene over Pt{111}.

[1] R. G. Windham, M. E. Bartram, and B. E. Koel, J. Phys. Chem. **92**, 2862 (1988).

[2] A. Cassuto, M. Mane, J. Jupille, G. Tourillon, and Ph. Parent, J. Phys. Chem. **96**, 5987 (1992).

[3] H. Steininger, H. Ibach, and S. Lehwald, Surf. Sci. **117**, 685 (1982).

[4] M. R. Smith, J. K. A. Clarke, G. Fitzsimons, and J. J. Rooney, Appl. Catal., A **165**, 257 (1997).

[5] F. Zaera, T. V. W. Janssens, and H. Ofner, Surf. Sci. **368**, 371 (1996).

[6] J. Stohr, F. Sette, and A. L. Johnson, Phys. Rev. Lett. **53**, 1684 (1984).

[7] M. Salmeron and G. A. Somorjai, J. Phys. Chem. **86**, 341 (1982).

[8] M. B. Hugenschmidt, P. Dolle, J. Jupille, and A. Cassuto, J. Vac. Sci. Technol. A **7**, 3312 (1989).

[9] E. M. Stuve and R. J. Madix, J. Phys. Chem. **89**, 3183 (1985).

[10] Q. Ge and D. A. King, J. Chem. Phys. **110**, 4699 (1999).

[11] U. Starke, A. Barbieri, N. Materer, M. A. Van Hove, and G. A. Somorjai, Surf. Sci. **286**, 1 (1993).

[12] C. L. Pettiette-Hall, D. P. Land, R. T. McIver, and J. C. Hemminger, J. Phys. Chem. **94**, 1948 (1990).

[13] W. Erley, Y. Li, D. P. Land, and J. C. Hemminger, Surf. Sci. **107**, 177 (1994).

[14] S. B. Mopshin, M. Trenary, and H. J. Robota, Chem. Phys. Lett. **154**, 511 (1989).

[15] J. L. Gland, F. Zaera, D. A. Fischer, R. G. Carr, and E. B. Kollin, Chem. Phys. Lett. **151**, 227 (1988).

[16] K. M. Ogle, J. R. Creighton, S. Akhter, and J. M. White, Surf. Sci. **169**, 246 (1986).

[17] K. Griffiths, W. N. Lennard, I. V. Mitchell, P. R. Norton, G. Pirug, and H. P. Bonzel, Surf. Sci. **284**, L389 (1993).

[18] J. N. Andersen, A. Beutler, S. L. Sorenson, R. Nyholm, B. Setlik, and D. Heskett, Chem. Phys. Lett. **269**, 371 (1997).

[19] J. Kubota, S. Ichihara, J. N. Kondo, K. Domen, and C. Hirose, Surf. Sci. **358**, 634 (1996).

[20] R. G. Windham and B. E. Koel, J. Phys. Chem. **94**, 1489 (1990).

[21] A. F. Lee, K. Wilson, A. Goldoni, R. Larciprete, and S. Lizzit, Surf. Sci. **513**, 140 (2002).

[22] A. F. Lee, K. Wilson, A. Goldoni, R. Larciprete, and S. Lizzit, Catal. Lett. **78**, 379 (2002).

[23] E. M. Patrito, P. Paredes Olivera, and H. Sellers, Surf. Sci. **380**, 264 (1997).

[24] B. E. Bent, C. M. Mate, C. T. Kao, A. J. Slavin, and G. A. Somorjai, J. Phys. Chem. **92**, 4720 (1988).

[25] J. McMurray, *Organic Chemistry*, 2nd ed. (Wadsworth, California, 1988).